

## IMPG1-c.847dup and Vitelliform Macular Dystrophy type 4: Multimodal Characterization and a Review of the Literature

Piero Barrera-Arshavin<sup>1\*</sup>, Eduardo Urrejola-Irarrazabal<sup>2</sup>, María J Rivas-Figueroa<sup>3</sup> and Juan I Verdaguer-Díaz<sup>3</sup>

<sup>1</sup>Ophthalmologist, Retina and Vitreous Fellowship, Fundación Oftalmológica Los Andes (FOLA), Chile.

<sup>2</sup>Ophthalmology Resident, Fundación Oftalmológica Los Andes (FOLA), Chile.

<sup>3</sup>Ophthalmologist-Retinologist at Fundación Oftalmológica Los Andes (FOLA), Chile.

### \*Correspondence:

Piero Barrera-Arshavin, Ophthalmologist, Retina and Vitreous Fellowship, Fundación Oftalmológica Los Andes (FOLA), Chile.

Received: 19 Mayr 2025; Accepted: 25 Jun 2025; Published: 03 July 2025

**Citation:** Piero Barrera-Arshavin, Eduardo Urrejola-Irarrazabal, María J Rivas-Figueroa, et al. IMPG1-c.847dup and Vitelliform Macular Dystrophy type 4: Multimodal Characterization and a Review of the Literature. *Med Clin Case Rep.* 2025; 5(1): 1-7.

### ABSTRACT

Adult-onset vitelliform macular dystrophy (AOVMD) encompasses several genetic entities. The autosomal-dominant subtype 4 is produced by heterozygous truncating variants in the *IMPG1* gene, leading to sialoprotein associated with the photoreceptor layer (SPACR) loss-of-function and haploinsufficiency.

**Case Report:** A 49-year-old woman presented with yellow photopsias and progressive visual loss, more pronounced in the left eye (OS). Spectral-domain optical coherence tomography disclosed ellipsoid-zone disruption with a sub-foveal deposit; fundus autofluorescence showed a hypo-fluorescent ring without the peripheral flecks typical of Stargardt disease. Full-field electroretinography revealed generalized rod-cone dysfunction without pathologic b-wave inversion. Targeted next-generation sequencing (330-gene panel) identified the pathogenic duplication *IMPG1-c.847dup*; no pathogenic variants were found in *ABCA4*, antiretinal antibodies were negative and systemic malignancy was excluded. During 14 months of follow-up, central foveal thickness declined by 24  $\mu\text{m}$  (3  $\mu\text{m}/\text{month}$ ) and visual acuity remained stable with low-vision rehabilitation.

**Discussion:** Clinical and imaging features match vitelliform macular dystrophy type 4 and differ clearly from autoimmune retinopathy, *ABCA4*-related Stargardt disease, *PRPH2*-linked maculopathy and hydroxychloroquine toxicity. Molecular confirmation obviated empirical immunosuppression, enabled accurate family counseling (50 % transmission risk) and may qualify the patient for forthcoming adeno-associated viral gene-therapy trials targeting *IMPG1* projected to start in 2026.

**Conclusion:** A single heterozygous frameshift duplication, *IMPG1-c.847dup*, is sufficient to cause AOVMD subtype 4. Integrating multimodal retinal imaging with next-generation sequencing provides a definitive diagnosis and supports personalized management.

### Keywords

IMPG1, Vitelliform macular dystrophy, Next-generation sequencing.

### Introduction

Hereditary retinal dystrophies are a group of progressive genetic diseases that affect visual function by compromising the structure and physiology of the photoreceptors (FR) and retinal pigment

epithelium (RPE) [1].

Vitelliform macular dystrophies (VMD) comprise a spectrum of inherited diseases characterized by yellowish subfoveal deposits and progressive visual loss. While most juvenile (Best) and part of the adult cases are explained by mutations in *BEST1* or *PRPH2*, up to 30% remained genetically undetermined [1,2].

---

Within this heterogeneous group, advances in genetic sequencing have allowed the identification of mutations in key genes that regulate the homeostasis of the extracellular environment of RFs, including the IMPG1 gene (Interphotoreceptor Matrix Proteoglycan 1, whose protein product, sialoprotein associated with the photoreceptor layer (SPACR), plays an essential role in the interphotoreceptor matrix (IPM) [1].

In recent cohorts, the overall prevalence of IMPG1/2 mutations in hereditary retinal dystrophies reaches 1.4-1.5% [3], but in adult-dominant VMD they account for ~3 % of BEST1/PRPH2-negative cases [3].

The IPM is a specialized extracellular network located between the FR outer segments and the EPR, which regulates critical functions such as cell adhesion, nutrient and metabolite transport, outer segment (SE) recycling, and intercellular biochemical communication [1,2]. The IMPG1 gene, predominantly expressed by FRs, encodes a structural glycoprotein with multiple functional domains, including SEA (Sperm protein, Enterokinase, Agrin) and Epidermal Growth Factor (EGF)-like domains, essential for interaction with other matrix macromolecules such as hyaluronan [1,3].

Mutations in IMPG1 have been associated mainly with two clinical phenotypes, vitelliform macular dystrophy (VMD) and autosomal dominant retinitis pigmentosa (ADRP). The type of mutation determines the clinical spectrum observed. In general, truncating or truncated mutations (such as frameshift and nonsense mutations) are associated with VMD, whereas missense mutations usually cause RPAD through negative dominant effect mechanisms [4,5].

The c.847dup variant consists of the duplication of a single base at position 847 of the IMPG1 gene. This addition shifts the reading frame starting at codon 283, so that seven incorrect amino acids are incorporated and then a stop codon appears prematurely. The result is a shortened protein that loses its function [3,6]. This type of mutation usually triggers cellular mechanisms of degradation of the mutated messenger RNA (mRNA) by "nonsense-mediated decay" (NMD), leading to a significant reduction of the functional protein product [7].

The pathophysiological consequence of this mutation is the structural disruption of the MPI due to the absence of functional SPACR. This protein, being absent or truncated, loses critical domains necessary for its localization and function, which alters the adhesion of photoreceptor outer segments to the EPR and affects the maintenance of the retinal microenvironment [1,3,8]. This alteration can lead to accumulation of lipofuscin or vitelliform material between the FRs and the EPR, a typical finding in VMD [4,9].

Clinically, patients with truncating mutations such as "c.847dup" have features compatible with adult vitelliform macular dystrophy, with onset in the second or third decade of life, moderately reduced

central vision, and subretinal vitelliform deposits visible on spectral domain (SD) optical coherence tomography (OCT), often with preservation of RPE integrity [5,9,10]. In contrast to severe forms of retinopathy associated with missense variants with negative dominant effect, phenotypes associated with haploinsufficiency loss of function usually have a slower and less aggressive course [6,11].

Cohort studies have documented that mutations such as "p.Arg507\*" and other truncated variants in IMPG1 generate a DMV-like phenotype when present in heterozygosis, suggesting that the underlying mechanism is haploinsufficiency, and not a toxic effect due to accumulation of misfolded protein [4,7]. On the other hand, missense mutations located in conserved regions of the SEA domains of SPACR can interfere with the native protein and generate more extensive pictures of retinal degeneration with progressive atrophy, as in autosomal dominant retinitis pigmentosa [6].

The clinical impact of the "c.847dup" variant has been reinforced by experimental studies in animal models. In knock-out mice for IMPG1, progressive retinal degeneration, disorganization of FR layers and accumulation of auto fluorescent material are observed, findings that reinforce the essential structural role of this protein in retinal homeostasis [1,8]. While these models do not always fully replicate the human phenotype, they support the notion that truncated variants in IMPG1 have clear pathogenic consequences in the retina.

From a diagnostic perspective, detection of c.847dup by targeted sequencing panels or clinical exome is highly relevant in patients with DMV phenotypes without mutations in classical genes such as BEST1, PRPH2 or ABCA4 [9,12]. The genotype-phenotype correlation is key in these cases to guide genetic counseling, the prediction of clinical evolution and the follow-up of at-risk relatives. The observation of bilateral vitelliform lesions on a preserved RPE, together with abnormal autofluorescent reflexes, constitutes a clinical diagnostic clue that should motivate genetic investigation of the IMPG1 gene [10,11].

Finally, it is important to mention that in certain cases dual or double mutation variants in retinal genes have been described, which poses challenges in the interpretation of the isolated pathogenic role of IMPG1. However, the finding of c.847dup in patients with classic DMV phenotype and the absence of other relevant variants in associated genes supports its primary role as a causative mutation [12].

In summary, the c.847dup variant (p.Ile283Asnfs\*7) of the IMPG1 gene is a frameshift mutation that produces a truncated and non-functional protein, compatible with a haploinsufficiency-mediated loss-of-function mechanism. This alteration compromises the architecture of the interphotoreceptor matrix, leading to the development of vitelliform macular dystrophy with progressive visual impairment.

Accurate diagnosis is clinically relevant because the phenotypic spectrum overlaps with autoimmune retinopathies, Stargardt disease (*ABCA4*), hydroxychloroquine toxicity and dominant *PRPH2* patterns. Clinical genomics allows etiological confirmation, guides family counseling and enables access to gene therapy trials in development, with cost-effectiveness impact demonstrated in real-world studies, described in ARVO 2024 [14,15].

We present the clinical-genetic characterization, 12 months of follow-up, of a Chilean patient heterozygous carrier of the truncating variant *IMPG1-c.847dup* (p.Ile283Asnfs\*7) and a review of the literature.

### Clinical Case

We present the case of a 49-year-old woman with no known morbid or ophthalmologic history, referred from the neuroophthalmology department after reporting a loss of visual acuity (VA) in the left eye (OS) during the process of renewing her driver's license.

The patient reported, a decrease in visual acuity (VA) in the OS since approximately five years ago, noticed by covering one eye. Since then, she perceives a slow but sustained progression of this loss, and currently the deterioration is greater and significant compared to previous years. Within the family history, she refers a maternal uncle with blindness secondary to an unspecified retinal disease.

At the initial ophthalmologic examination, uncorrected VA in the right eye (OD) 0.33 with correction. The VA in the OD was hand motion (HM), with no improvement with correction. Intraocular pressure (IOP) was 16 mmHg in both eyes. Ocular motility examination was normal, with preserved direct and consensual pupillary reflexes bilaterally. Biomicroscopy (BMC) revealed formed anterior chamber, without inflammatory signs, iris without alterations and transparent lens.

The fundus examination of the OD was normal, whereas in the OS there was a macular granular appearance with a slight cellophane-like sheen and faint hypopigmented subretinal lesions in the inferior temporal arcade. Macular optical coherence tomography (OCT) showed a subfoveal alteration of the ellipsoid, more marked in the OS. Autofluorescence (AF) showed hypoautofluorescence rings at macular level in the same eye. (Figure 1).

A possible evanescent white dot syndrome (MEWDS) was hypothesized as a diagnosis and a referral was made to a retina and uvea specialist for a second opinion.

In the second evaluation, one month later, the patient reported that the visual loss in the OS was accompanied by a decrease in central vision in the OD, accompanied by an alteration in the perception of colors and photopsias, described as yellow lights or spots when closing the eyes. In addition, he reported seeing better at night and described vision with the OD as "gray".

On examination, VA of 0.1 in OD the fundus and HM in the OS,

with IOP within normal limits. The fundus of the OD showed bright optic nerve head an macula with physiologic excavation, in addition to mild peripheral pigmentary scatter greater in the OS. Hereditary retinal dystrophy or autoimmune retinitis (AIR) was suspected. Complementary studies were indicated including electroretinogram (ERG), Goldman campimetry (GVC), OCT, Farnsworth D-15 test and fundus photography, tests to exclude infectious pathology such as syphilis, tuberculosis, which were ruled out, and otherwise systemic study to rule out neoplastic cause.

In the following control, the examinations showed a central scotoma in the OD in the GVC (Figures 2, 3) and diffuse alteration in color perception (Figure 4). The ERG showed mild to moderate generalized alteration in the OD and severe in the OS, with a flat tendency in rods (Figures 5,6). OCT revealed involvement of the outer retina in both eyes with a macular thickness of 169  $\mu\text{m}$  (Figures 7,8). Given the bilateral progression, initially unilateral, and the functional pattern compatible with photoreceptor degeneration, the hypothesis of an autoimmune versus hereditary etiology was reinforced, and the case was presented to an expert in oculogenetics, who suggested complementing the study with a basic genetic panel, and complementary through genomic sequence and exome, (invitae, labcorp) [16] (Figure 9).

The patient reported further visual decline, with more blurred vision and frequent presence of yellow "moons" type lights in the OD. VA in the OD was 0.2 and in the OS light perception. BMC remained normal. The fundus of the OD showed signs of peripheral chorioretinal atrophy, while the fundus of the OS persisted with very faint pigmentary dispersion. The result of the genetic panel revealed a pathogenic mutation in the *IMPG1* gene, a finding compatible with autosomal recessive macular dystrophy, with no known association to autosomal dominant inheritance. The patient was referred to the visual rehabilitation unit (VRU) for follow-up and management.



**Figure 1:** Blue-light autofluorescence (Spectralis, 30° and 55°). (A) Right eye, field 35°: macular hypoautofluorescent ring with faint hyperautofluorescent rim; periphery without flecks.

- (B) Right eye, field 55°: confirms ring pattern and absence of perifoveal deposits.
- (C) Left eye, field 30°: more irregular hypo-AF ring with discrete central hyper-AF signal; no peripheral flecks.
- (D) Left eye, field 55°: macular hypo-/hyper-AF mottling and lesion-free periphery.

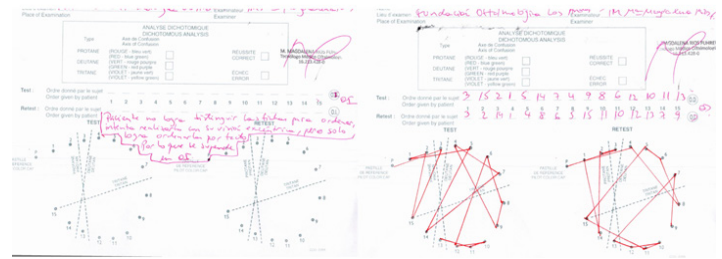


Figure 4: Farnsworth D-15 color test.

**Left panel:** left eye; the patient failed to sort the cards by hue, so the examiner stopped the test after several attempts. This indicates a severe disturbance, with no specific axis of confusion.

**Right panel:** right eye; there is a disorganized pattern with multiple crosses crossing the protan, deutan and tritan axes, compatible with global dyschromatopsia rather than an isolated chromatic defect.

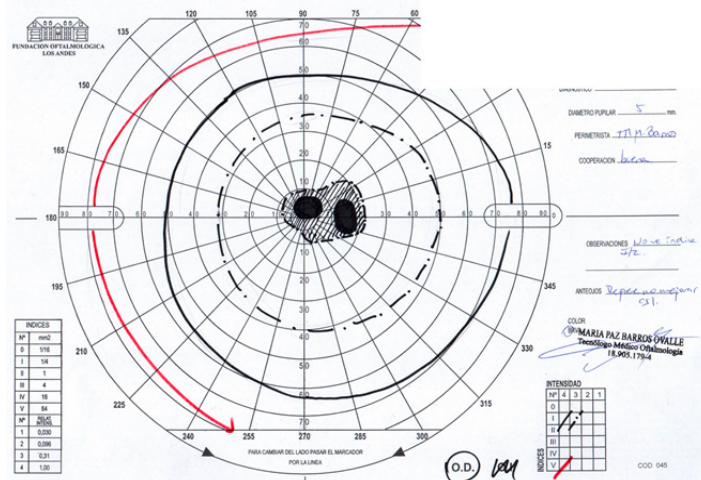


Figure 2: Goldmann campimetry (GVC), right eye.

Plotted with stimuli III-4e (solid line) and V-4e (thick red line as a theoretical limit). There is a dense central scotoma of 4-5° (shaded area) accompanied by a ring of relative depression affecting approximately the first 25° of the field, more pronounced in the nasal meridians. The peripheral boundary with III-4e stimulus is preserved around 60-65° and the V-4e intensity isothera reaches 70-75°, indicating preservation of the far peripheral field.

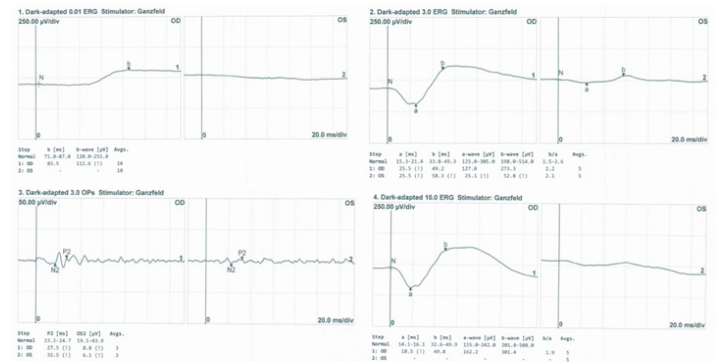


Figure 5: Full-field electroretinogram.

Upper left panel: rod stimulus 0.01 (response almost extinguished in RO). Upper right panel: combined 3.0 stimulus with b-wave reduced 40% in OD and >80% in OI, without electronegativity. Lower left panel: oscillatory potentials (OPs) with decreased amplitude P2 in both eyes, more marked in OI. Lower right panel: bright flash response 10.0, confirming diffuse cone-shaped rod depression.

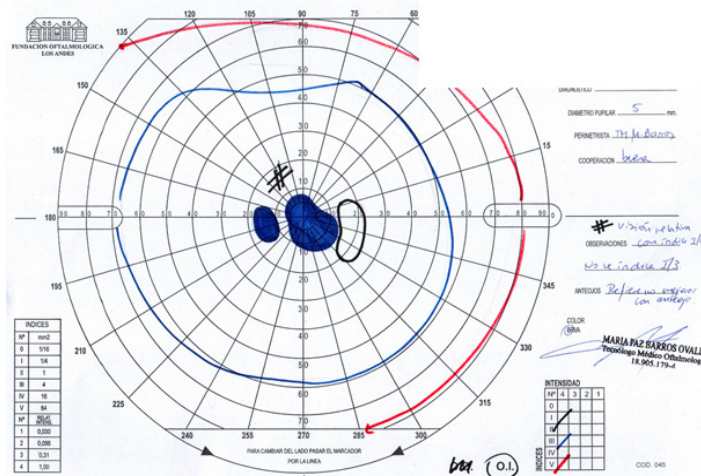


Figure 3: Goldmann campimetry (GVC), left eye.

Isoptera recorded with stimulus III-4e (blue trace) shows a concentric restricted field approaching 40-45° in most meridians, with somewhat more respect for the temporal quadrants. A dense central scotoma of about 5° and a nasal paracentral scotoma (shaded areas) are seen. With V-4e stimulus (theoretical limit in red) the global field extends to 70-75°, confirming relative preservation of the peripheral retina.

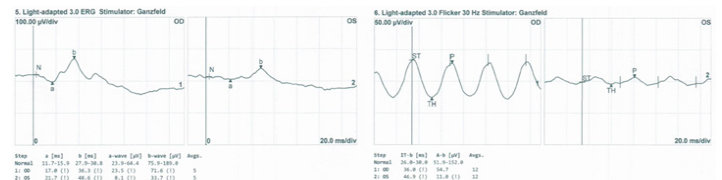
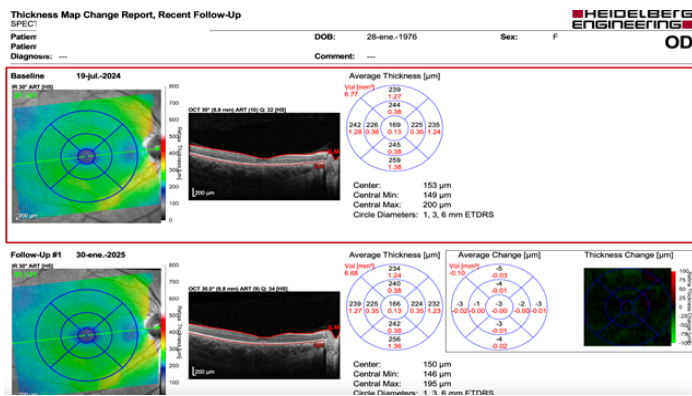


Figure 6: Photopic electroretinogram.

Left: isolated 3.0 cone stimulus; the right eye maintains 71 μV b-wave (-40% with respect to the lower limit) with prolonged latency, while the left eye exhibits severely reduced amplitude (34 μV) and longer delay. Right: 30 Hz flicker with the same stimulus (cone function recording only). The right eye shows a moderate decrease in amplitude (≈ 55 μV) and latency of 36 ms; the left eye exhibits nearly extinguished response (11 μV) and latency of 47 ms.



**Figure 7:** Quantitative tracking of macular thickness by OCT-Spectralis, right eye.

Follow-up, the map indicates mild reductions of 3 - 4 µm in most quadrants. These findings document an average foveal thinning of = or < 3 µm/month.

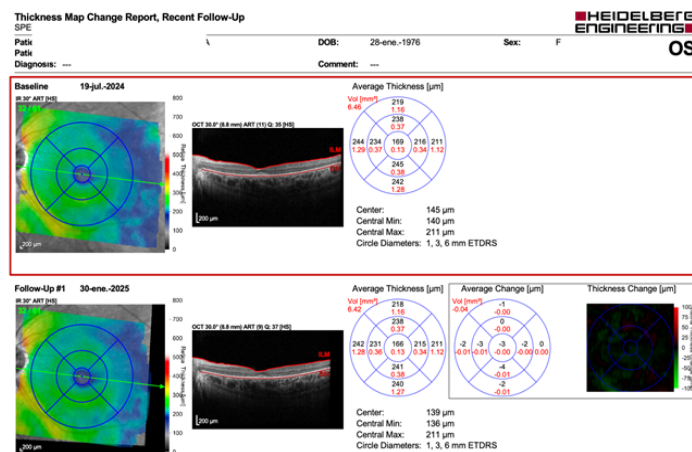


**Figure 8:** Quantitative tracking of macular thickness by OCT-Spectralis, left eye.

The map shows discrete reductions of 2-4 µm. The mean foveal decrease (0.4 µm/month) confirms a slightly slower course than that observed in the right eye.

GENE	VARIANT	ZYGOSITY	VARIANT CLASSIFICATION
IMPG1	c.847dup (p.Ile283Asnfs*7)	Heterozygous	Pathogenic (classified variant)

**About this test**  
This diagnostic test evaluates 330 gene(s) for variants (genetic changes) that are associated with genetic disorders. Diagnostic genetic testing, when combined with family history and other medical results, may provide information to clarify individual risk, support a clinical diagnosis, and assist with the development of a personalized treatment and management strategy.

**Figure 9:** Genetic outcome (330-gene panel for inherited retinal disorders, Invitae).

A single pathogenic variant was identified in IMPG1: c.847dup duplication causing p.Ile283Asnfs\*7 frameshift. The variant was found in heterozygosity and was classified as pathogenic according to ACMG criteria. No other relevant alterations were detected in the remaining 329 genes.

**Table 1:** Summary chronology of the case.

Date	Most relevant clinical findings	Testing / Driving
05-Jun-24	Blurred vision OI; VA 0.12/PL	OCT-SOLIX: ellipsoid band disruption
19-Jul-24	Persistent photopsias; scotoma OD	CVG + ERG: cone-sticks ↓ (severe OI).
07-Jan-25	Macular progression OI; VA 0.25/0.05	OCT-Spectralis (169 → 150 µm)
02-May-25	Heterozygous <i>IMPG1</i> c.847dup variant	Invitae Report* [16]
May-25 - act.	Stable with visual aids	OCT and CV every 6 months

**Table 2:** Multimodal findings analysis.

Modality	Result	Interpretation
OCT	Ellipsoid band foveal disruption, hyperreflective deposits, early subfoveal thickening followed by central thinning to 150 µm	Typical VMD-IMPG1 AD pattern
AF	Hypohyper annular mottling without perifoveal "flecks".	Differs from <i>ABCA4</i> ; consistent with adult VMD
ERG ISCEV	OD: b-wave amplitude 45 µV (↓40%); OI: b-wave 15 µV (↓80%); latencies +10 ms; flicker 30 Hz 45 % ↓	Diffuse rod-cone dysfunction described in VMD4; non-electronegative → against AIR.
CVG	Centric scotoma OD, moderate concentric defect OI	Compatible with macular loss and slow peripheral involvement.
Genetics	<i>IMPG1-c.847dup</i> heterozygous; remainder of panel negative	Haploinsufficiency dominant; rules out recessive IRD (incl. <i>ABCA4</i> )
Serologies / PET-CT	Anti-recoverin, TRPM1 -; PET-CT normal	Reduces likelihood of paraneoplastic retinopathy

OCT = optical coherence tomography; AF = autofluorescence; ERG ISCEV = full-field electroretinogram according to International Society for Clinical Electrophysiology of Vision protocol; GVC = Goldmann campimetry; OD/OS = right/left eye; µm = micrometers; VMD-IMPG1 AD = autosomal dominantly inherited *IMPG1-associated* vitelliform macular dystrophy; *ABCA4* = *ATP-binding cassette sub-family A member 4* gene; AIR = autoimmune retinopathy; PET-CT = positron emission tomography combined with computed tomography; IRD = inherited retinal dystrophies; TRPM1 = *Transient Receptor Potential Melastatin 1*; ↓ = decrease.

**Table 3:** Diagnostic performance of different next generation sequencing (NGS) strategies in hereditary retinal dystrophies (IRD).

NGS Strategy	Genes analyzed	Case resolution rate
Directed panel	200 - 350	60 - 70% [18]
Clinical exome	≈ 20 000	55 - 65%* (similar to panel; higher capacity for rare genes) [19]
Whole genome (WGS)	Whole genome	65 - 80% when including duplications/deletions and deep intronic variants [20]

\*Percentage of patients in whom the causative variant(s) are identified. NGS = next-generation sequencing; IRD = *inherited retinal dystrophies*; WGS = whole-genome sequencing.

## Discussion

Regarding the molecular mechanism and phenotypic correlation, it is worth mentioning that "c.847dup" introduces a stop codon prematurely generating p.Ile283Asnfs\*7 and nonsense-mediated decay. Cell models show a 60% decrease in SPACR, altering outer segment adhesion and triggering vitelliform deposits [3]. AD families with truncated IMPG1 debut between 30-50 years, slow course and variable cone-rod ERG, features reproduced in our patient [6].

The impact of clinical genetics in hereditary retinal dystrophies (IRD), the diagnostic yield through next-generation sequencing (NGS) exceeds 65%; it provides prognosis, trial eligibility for clinical trials and family counseling [17-20]. (Table 3).

Cost-utility studies estimate savings of  $\geq$  US\$ 4500 per patient by avoiding repeated diagnostic tests and unnecessary treatments [14]. The molecular finding avoided the establishment of chronic immunotherapy and, in addition, made it possible to attribute the OD/OS clinical asymmetry to the variability of expression characteristic of autosomal dominant mutations, a phenomenon described even among siblings carrying the same variant [3].

Table 4 summarizes the clinical and molecular features that distinguish VMD4-IMPG1 from the other entities considered as differential diagnoses. Our case coincides with the first column: debut at 49 years of age, heterozygous frameshift mutation, absence of inflammation, rod-cone dysfunction without electronegativity and AF in hypo-AF ring. These findings contrast sharply with the other four possibilities:

Autoimmune retinopathy (AIR) [21]. A typical presentation includes photopsias followed by acute hemeralopia in patients aged 50-70 years, electronegative ERG (b/a inversion) and often linear or diffuse AF mottling. The negativity of our anti-retinal antibodies (recoverin, TRPM1) and neoplasia-free PET-CT, together with the absence of electronegativity, strongly disprove this hypothesis.

**Table 4:** Differential diagnoses.

Feature	VMD4-IMPG1	AIR	Stargardt ABCA4	VMD-PRPH2	HQ Toxicity
Typical mutation	Frameshift heterozygous	ARAs (recoverin/TRPM1)	ABCA4 Byalelic	Missense PRPH2	-
Debut age	30-50 a	50-70 a	< 30 a	40-60 a	> 7 to HQ use
Symptoms	Photopsias, dyschromatopsia	Photopsias + acute hemeralopia	Slow central scotoma	Fluctuating vision	Perifoveal scotoma
Inflammation	Absent	$\leq$ 1+ vitreous	Absent	Absent	Absent
ERG	Rod-cone $\downarrow$ (not EN)	EN b/a $\downarrow$	Early cone	Early cone	Flicker $\downarrow$
AF	Hypo-AF ring	Diffuse linear mottling	Flecks hyper-AF pisciforms	Lattice pattern	Bulls eye ring
Peripheral HF	Normal	Variable	Fuzzy Flecks	Reticular mottling	Normal
Response to immunosuppression	-	Improves/stabilizes	-	-	HQ Suspension

**VMD4-IMPG1** = vitelliform macular dystrophy type 4 associated with dominant mutations in *IMPG1*; **AIR** = autoimmune retinopathy; **ABCA4** = *ATP-binding cassette sub-family A member 4* gene (Stargardt's disease); **PRPH2** = *Peripherin-2/RDS* gene (dominant vitelliform maculopathy); **HQ** = hydroxychloroquine; **ARAs** = anti-retinal autoantibodies (recoverin, TRPM1, etc.); **a/ b-wave** = ERG principal components; **EN** = electronegative; **AF** = autofluorescence; "bull's-eye" = hyper/hypo-AF ring pattern typical of HQ toxicity;  $\downarrow$  = decrease.

Stargardt's disease (ABCA4) [22]; onset is usually in those younger than 30 years and FA shows hyper-AF pisciform flecks extending to the periphery; in addition, ERG first affects cones. Our NGS panel was negative for pathogenic ABCA4 variants and FA lacks flecks, ruling out this entity.

VMD due to PRPH2 [23], shares the age of onset, but is usually associated with dominant missense mutations and a reticular or pseudohypopyon PA pattern; vision fluctuates with accumulation/reabsorption of vitelliform material. In our patient, the mutation in IMPG1, the ring FA and the relatively linear evolution differ from the classic PRPH2 phenotype.

Hydroxychloroquine toxicity [24], more than 5 to 7 years of exposure is required; FA shows a peri-foveal bullseye ring and ERG preferentially affects the flicker. The patient never used hydroxychloroquine and the perifoveal FA is normal; the diagnosis is ruled out according to the AAO criteria, and to the directed anamnesis.

Thus, the combination of (i) heterozygous truncated IMPG1-c.847dup mutation, (ii) ring autofluorescence without flecks, (iii) non-electron-negative rod-cone dysfunction and (iv) absence of inflammation or neoplasia, positions the picture within the VMD4-IMPG1 spectrum, confirming that the OD/OS asymmetry reflects the dominant expression variability described even among members of the same family. Therapeutically, adeno-associated vectors (AAV-IMPG1) under pre-clinical testing in rodents show rescue of ellipsoid thickness and ERG preservation at 6 months, with Investigational New Drug (IND) research planned for 2026 [2].

The literature describes mean VA decrease 0.05 LogMAR/year and macular atrophy  $< 40 \mu\text{m}/\text{year}$  in VMD4. Our patient's loss of  $24 \mu\text{m}$  in 14 months is consistent with a "moderately progressive" course. Biannual follow-up with OCT/AF and CVG, job counseling and eventual gene therapy once available is recommended.

## Conclusion

The frameshift duplication of the *IMPG1-c.847dup* gene, even in heterozygosity, is sufficient by itself to cause vitelliform macular dystrophy type 4 through a haploinsufficiency mechanism, which underlines the importance of not automatically labeling every patient with a single affected allele as a "carrier". The combination of OCT, FA and ERG, analyzed in an integrated manner with the results of next-generation sequencing, makes it possible to accurately discriminate autosomal dominant dystrophies (AD) from autoimmune retinopathies (ARI) and, consequently, to dispense with empirical immunotherapy. During follow-up, foveal thinning progressed slowly, approximately 3 µm per month, which is in agreement with previous series and supports the strategy of biannual structural controls together with early visual rehabilitation. Finally, the development of AAV vectors targeting *IMPG1* makes accurate genotypic confirmation imperative to ensure timely access of patients to future gene-specific interventions.

## References

1. Olivier G, Brabet P, Pirot N, et al. SPACR Encoded by IMPG1 Is Essential for Photoreceptor Survival by Interplaying between the Interphotoreceptor Matrix and the Retinal Pigment Epithelium. *Genes*. 2022; 13: 1508.
2. Manes G, Meunier I, Avila-Fernandez A, et al. Mutations in IMPG1 Cause Vitelliform Macular Dystrophies. *Am J Hum Genet*. 2013; 93: 571-578.
3. Chan L, Adams M, Aleman TS, et al. Intrafamilial variability of IMPG1-associated vitelliform dystrophy. *Retin Cases Brief Rep*. 2025.
4. Meunier I, Manes G, Bocquet B, et al. Frequency and Clinical Pattern of Vitelliform Macular Dystrophy Caused by Mutations of Interphotoreceptor Matrix IMPG1 and IMPG2 Genes. *Ophthalmology*. 2014; 121: 2406-2414.
5. Venselaar H. IMPG1 variant causes autosomal dominant retinitis pigmentosa; revision of the benign concentric annular macular dystrophy phenotype. *J Med Genet*. 2021; 58: 570-578.
6. Brandl C, Schulz H, Charbel Issa P, et al. Mutations in the Genes for Interphotoreceptor Matrix Proteoglycans, IMPG1 and IMPG2, in Patients with Vitelliform Macular Lesions. *Genes*. 2017; 8: 170.
7. Bandah-Rozenfeld D, Collin RWJ, Banin E, et al. Mutations in IMPG2, Encoding Interphotoreceptor Matrix Proteoglycan 2, Cause Autosomal-Recessive Retinitis Pigmentosa. *Am J Hum Genet*. 2010; 87: 199-208.
8. Wolfram L, Merle DA, Kühlewein L, et al. Clinical manifestations of dual-gene variants involving ABCA4 in retinal dystrophies. *BMC Ophthalmol*. 2025; 25: 239.
9. Habibi I, Falfoul Y, Tran HV, et al. Different Phenotypes in Pseudodominant Inherited Retinal Dystrophies. *Front Cell Dev Biol*. 2021; 9: 625560.
10. Olivier G, Quiles M, Andreo E, et al. Functional consequences of IMPG1 deficiency: insights from knockout models. *Genes*. 2022; 13: 1508.
11. Meunier I, Zanlonghi X, Le Meur G, et al. Imaging findings in IMPG1-related vitelliform maculopathy. *Ophthalmology*. 2014; 93: 571-578.
12. Manes G, Dhaenens CM, Ayuso C, et al. Spectrum and expressivity of IMPG1 variants in retinal dystrophies. *Am J Hum Genet*. 2013; 16: 43.
13. Weisschuh N, Kohl S, Wissinger B, et al. Genetic diagnostic value of IMPG1 in unexplained macular dystrophies. *BMC Ophthalmol*. 2025.
14. Zhang Q, Qian C, Kirsten L, et al. Economic value of early genetic testing in inherited retinal dystrophies diagnosis. *Association for Research in Vision and Ophthalmology*. 2024.
15. De Silva T, Ginton S, Lipkova V, et al. Deep Learning based Algorithm for Automatic cRORA and Photoreceptor Loss Detection in SD-OCT Imaging. *Association for Research in Vision and Ophthalmology*. 2024; 65: 2770.
16. Robert C, Jonathan B, Wayne G, et al. ACMG recommendations for reporting of incidental findings in clinical exome and genome sequencing Green. *Genetics in Medicine*. 2013; 15: 565-557.
17. Nebbioso M, Artico M, Gharbiya M, et al. State of the Art on Inherited Retinal Dystrophies: Management and Molecular Genetics. *J Clin Med*. 2025; 14: 3526.
18. Stone EM, Jeanen A, Scott W, et al. Genetic testing for inherited eye disease: findings in 1000 consecutive families. *Am J Hum Genet*. 2017; 100: 285-292.
19. Ellingford JM, Stephanie B, Sanjeev B, et al. Whole-genome sequencing increases diagnostic yield in inherited retinal disease: a cohort study. *J Med Genet*. 2016; 53: 286-292.
20. Wang F, Laura W, Pete H, et al. Deep intronic and structural variants boost the diagnostic rate of inherited retinal dystrophies. *Hum Genet*. 2023; 142: 235-246.
21. Modjtahedi BS, Palestine A, Jampol LM, et al. Guidelines for the diagnosis of autoimmune retinopathy. *Ophthalmology Retina*. 2025; 9: e1095-e1108.
22. Fujinami K, Aukrust I, Jansson RW, et al. Clinical and molecular characteristics of ABCA4-related disease. *Prog Retin Eye Res*. 2019; 72: 100759.
23. Saxena S, Paavo M, Chen L, et al. Multimodal imaging in vitelliform dystrophies. *Surv Ophthalmol*. 2022; 67: 232-249.
24. Marmor MF, Kellner U, Y La T, et al. Recommendations on screening for chloroquine and hydroxychloroquine retinopathy. *Ophthalmology*. 2020; 127: 117-128.